

Study on Thermal Coupling Characteristics of Constrained Blades Based on Spin Softening

ZHAO Huiying, MEN Xiuhua^{*}, CUI Huanyong and ZHANG Kun

School of Mechanical Engineering, University of Jinan, Jinan, 250022, China

Tel.: +8618363033060

E-mail:772632281@qq.com

Received: 22 July 2016 /Accepted: 22 August 2016 /Published: 31 August 2016

Abstract: The effects of spin softening and thermal shock had important influence upon the structural stability of blades in rotary machinery. Based on the theories of rotor dynamics and thermodynamics, a dynamic model of rotating blade was built. Considering the effect of spin softening, the research on vibration characteristics of high speed rotating blades was carried out under the centrifugal field and thermal coupling. The results had demonstrated that frequency of blade vibration increases with rising rotating velocity due to the effect of centrifugal force, whilst the frequency of all orders declined with the influence of thermal coupling. The conclusion derived from this paper had both theoretical and empirical value on retrofitting, optimal-designing, as well as engineering application for high speed rotating blades. Copyright © 2016 IFSA Publishing, S. L.

Keywords: Rotating machinery, Blade, Spin softening, Thermal coupling, Vibration.

1. Introduction

Blades are the key components of aero-engine. Due to the effect of mechanical excitation and heat flow field, the rotating blade can produce obvious vibration response on the process of engine operation. Meanwhile, the spin softening effect and thermal shock load from operating environment would increase the rotating shape of blade, furtherly affecting the overall performance of engine and flight safety [1]. Therefore, studying the vibration characteristics of rotating blades and analyzing the blades reliability are of great significance to improve the performance of engine and to reduce the damage from the nonlinear vibration.

Considering complex operating ambient of high-speed rotation blade, it's difficult to obtain the vibration characteristic of centrifugal field, temperature field, etc. using experimental methods. Therefore, a simulating approach based on dynamics

theory becomes to be important for getting vibration characteristics of blades in actual operating state of aircraft engines. In recent years, many scholars have done some researches on how to enhance the dynamic stability of high speed rotating blades. For natural vibration characteristics of blades, Saravia took the rotating blades as thin-walled structure, and applied finite element method to analyze its free vibration and dynamic stability [2]. Diken [3] proposed vibration differential equation of the blade-rotor coupling system derived from Lagrange equation. And then the dynamic characteristic of coupled system with eccentric mass was studied in consideration of periodic time-varying coefficient. For certain aero-engine turbine blades, Chunwang Li made research on the vibration modal analysis to get influences from various factors on blades including centrifugal force field, aerodynamic field, temperature field and thermal field etc. [4]. For thermal deformation of blades in vibration state, Sun Qiang made a study on vibration

characteristics caused by constant temperature field, but did not take into account the change of mechanical properties and thermal stress field due to different temperature distribution of blade [5]. In literature, a modal analysis of T leaf blade was made under the action of centrifugal and temperature, but the spin softening was ignored completely by researchers [6]. Obviously, when the blade rotates in state of high speed, the rotational softening effect and thermal load can affect vibration characteristics of blades together, and now little research was focused on this common influence for blades.

In this paper, a spin softening model of rotating blade was firstly established for high speed rotating blades, and the modal analysis in centrifugal field and thermal field was carried out to investigate blade deformation. The obtained conclusion could provide technical guidance for fault research and optimization design of high speed rotating blades.

2. Coupling Model of Constrained Blades

2.1. Spin Softening Model of Spring-mass System

In practical, the rotating blade is a constrained elastomer. During rotation, the elastomer is subjected to the action of centrifugal force and can produce obvious longitudinal displacement. According to this feature, the physical model of rotating blade can be simplified into a spring-mass system, as shown in Fig. 1. The spring rotates around Q axis with a mass of M on the other side of the shaft [7]. When the mass M is fixed, the large longitudinal deformation produced in rotating state can change the stiffness of elastomer, thus affecting the frequency and deformation of whole model. This phenomenon is called as spin softening.

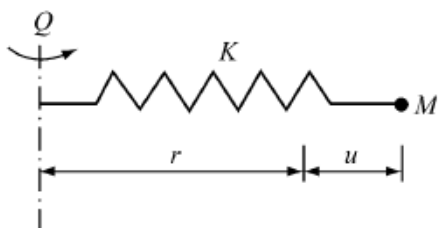


Fig. 1. The physical model of rotating blade.

As shown in Fig. 1, the parameter of u is the deformation amount of spring relative to free position, and the r is original length of spring. When the spring rotates at low speed, the deformation is small and the change of u can be negligible. So the equation of motion is given as:

$$Ku = \Omega^2 Mr \quad (1)$$

where K is the spring stiffness, Ω is the rotational angular velocity, r is also called as the radius of free position of the particle relative to the axis.

In high speed rotation, the rotational softening effect is intensified, and the deformation of spring becomes larger. In that case, the change of u can make important influence on the whole load balance. The equation of motion changes into:

$$Ku = \Omega^2 M(r + u) \quad (2)$$

By formula (1) and (2), the new equation can be obtained:

$$(K - \Omega^2 M)u = \Omega^2 Mr \quad (3)$$

Set $\bar{K} = K - \Omega^2 M$, the formula (3) is expressed as:

$$\bar{K}u = \Omega^2 Mr \quad (4)$$

From (4), it is found that the stiffness \bar{K} is smaller than original stiffness of K . When other parameters are fixed, the change of stiffness could affect the motion equation of structural vibration directly.

2.2. Vibration Equation of Thermal Coupling for Blade

In the rotating state, the constrained blade can produce obvious structural vibration. Applying Hamilton principles, the motion Equation is derived as [8]:

$$M\ddot{X}(t) + M_G\dot{X}(t) + KX(t) = F, \quad (5)$$

where $X(t)$, $\dot{X}(t)$, $\ddot{X}(t)$ are the displacement vector, speed vector and acceleration vector, respectively; M is the mass matrix; M_G is the damping matrix; K is the stiffness matrix; F is the periodic external excitation force.

Due to effect from centrifugal force field and temperature field, the blade can produce stress stiffening phenomenon, with additional stiffness matrix appearing. In this case, the stiffness matrix in formula (5) is bound to change. Set the initial stiffness matrix of blade as K_0 . The K_c and K_t are denoted as the additional stiffness matrix generated from centrifugal force field and temperature field, respectively. Without regarding to the influence of periodic external excitation force and damping, the non-damping free vibration equation can be derived from Eq. (5) as:

$$M\ddot{X}(t) + (K_0 + K_c + K_t)X(t) = 0 \quad (6)$$

For high speed rotating blade, spin softening effect can change the stiffness matrix of equation.

Therefore, the blade vibration equation is change into:

$$M\ddot{X}(t) + (K_0 + K_c + K_t - \Omega^2 M)X(t) = 0, \quad (7)$$

where, $\Omega^2 M$ is the spin softening matrix. Compared with the formula (6) and formula (7), it can be seen that there is a reduction of the stiffness matrix of the whole motion system due to existence of softening effect.

By working out the feature equation, the natural frequency and model shape are obtained, and detailed relationship can be represented as:

$$f_i = \frac{1}{2\pi} \sqrt{\frac{K_i}{M_i}}, \quad (8)$$

where, f_i is the natural frequency of the structure, K_i is the structure stiffness, M_i is the structure mass, with $i=1, 2, 3, \dots, n$.

3. The Modal Analysis of Blade

Select certain type of high speed rotating blade to analyze its modal feature. The material of blade was high temperature alloy K4002, with density of $8.5 \times 10^3 \text{Kg/m}^3$. Other material parameters at different temperature were shown in Table 1. The blade was connected with the wheel disc. Disc material was steel with density of $7.8 \times 10^3 \text{Kg/m}^3$. Detailed material parameters of disc were shown in Table 2.

Table 1. Mechanical parameters of K4002 with different temperature.

Parameter	20 °C	100 °C	300 °C	500 °C	700 °C	900 °C
$E(10^9 \text{N/m}^2)$	194	188	181	169	156	149
γ	0.223	0.204	0.206	0.190	0.199	0.286
$\lambda \text{ (W/(m} \cdot \text{°C))}$	—	—	8.79	10.47	14.24	18.42
$\alpha (10^{-5}/\text{°C})$	—	1.23	1.29	1.34	1.41	1.51

Table 2. Mechanical parameters of steel with different temperature.

Parameter	20 °C	100 °C	300 °C	500 °C	700 °C	900 °C
$E(10^9 \text{N/m}^2)$	209	202	187	175	129	77
γ	0.269	0.270	0.312	0.308	0.301	0.285
$\lambda \text{ (W/(m} \cdot \text{°C))}$	—	10.05	12.98	16.33	20.52	24.28
$\alpha (10^{-5}/\text{°C})$	—	1.26	1.29	1.34	1.42	1.55

Where E is the elastic modulus, γ is the Poisson ratio, λ is the thermal conductivity, α is the coefficient of thermal expansion.

3.1. The Vibration Characteristics of Blade Under the Centrifugal Force Field

One blade of the whole model was selected to establish finite element model using ANSYS. The blade was divided into 1479 units and 3120 nodes by using shell element SHELL181. For the disc, 8 node solid185 was adopted to divide elements with 83612 units and 15806 nodes, as shown in Fig. 2.

Only considering the rotational softening effect, a modal analysis was realized under the action of centrifugal force field. In this case, the stiffness of K_c and K_0 were not zero, and the stiffness of K_t was equal to zero. So, the formula (7) could be derived as again:

$$M\ddot{X}(t) + (K_0 + K_c - \Omega^2 M)X(t) = 0 \quad (9)$$

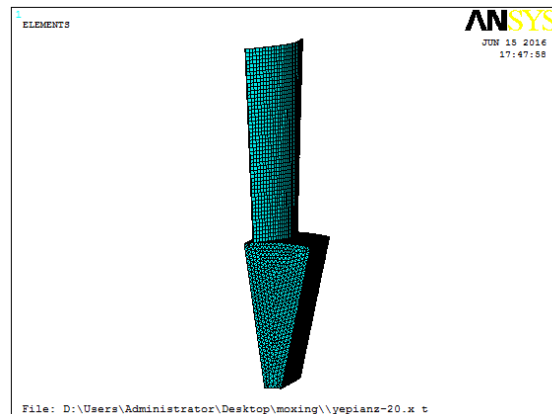


Fig. 2. The finite element model of blade.

In the solving model, the ambient temperature was set as 20 °C, and cyclic symmetry constraint was

applied on both sides of blade. According to the rotational speed of turbine shaft, different angular velocity of Z axis was loaded on the blade, with 500 rad/s, 700 rad/s, 1000 rad/s and 1200 rad/s, respectively. To obtain the centrifugal stress of blade,

a static analysis was carried out firstly. Then converting centrifugal stress to prestress, the modal analysis was realized based on the equation of motion (8). Finally, we could get the frequency and vibration mode of blade at first 5 orders, as shown in Table 3.

Table 3. Vibration mode of blade under the centrifugal force.

Order	Mode	Order (hz) (n=0)	Mode	Order (hz) (n=500)	Mode	Order (hz) (n=700)	Mode	Order (hz) (n=1000)	Mode	Order (hz) (n=1200)
1	T	328.31	T	348.24	T	366.35	T	402.19	T	430.79
2	B	589.54	B	598.90	B	607.71	B	625.91	B	641.12
3	T&B	1439.5	T&B	1474.8	T&B	1507.8	T&B	1575.7	T&B	1631.9
4	T&B	2137.2	T&B	2147.2	T&B	2155.6	T&B	2170.8	T&B	2182.0
5	T&B	2257.2	T&B	2275.5	T&B	2294.0	T&B	2335.2	T&B	2371.8

Note: n- the rotational speed of blade, rad/s; T- torsion; B- bending.

It can be seen from the Table 3 that the natural frequency of blade was closely related to rotating speed. For the same order, the natural frequency of blade could increase with the increase of rotational speed. Taking the first order as example, when the rotational speed raised from 0 rad/s to 1200 rad/s, the natural frequency changed from 328.31 Hz to 430.79 Hz, with the change range of 31.2 %. The reason was that a greater radial centrifugal force of wheel could be generated due to increased rotational speed, and the stiffness matrix of blade would become larger correspondingly. Meanwhile, the frequency of structure was proportional to structure stiffness, so the frequency was bound to change with increase of rotational speed. On the other hand, the frequency range of blade could be expanded due to the increase of rotational speed, and the resonance of whole structure should be avoided to reduce the amplitude of structural deformation and engine trouble.

Meanwhile, we could see that the change of each mode shape of blade was not very large at different speed. The first mode was the torsional vibration along Y axis with smaller change, and the second mode was the bending vibration along X axis. From the third to sixth modes, the blade generated a combination of bending and torsion along X and Y axis.

Because of the smaller gap between the aero-engine blade tip and the inner wall of machine box, the tip and the casing was prone to rub-impact on high-speed operation. Researches had shown that the radial deformation along X axis of blade was one of the important factors in the process of rub-impact. In order to study the detailed change of radial deformation, a parameter of τ was introduced to represent the relative deformation degree of along the X axis at different rotating speed.

$$\tau = \frac{\delta - \delta_0}{\delta_0} \times 100\% \quad (10)$$

where δ is the amplitude of deformation along the X axis; δ_0 is the amplitude of deformation along the X axis when the frequency was equal to zero. The detailed deformation degree of τ was shown in Fig. 3.

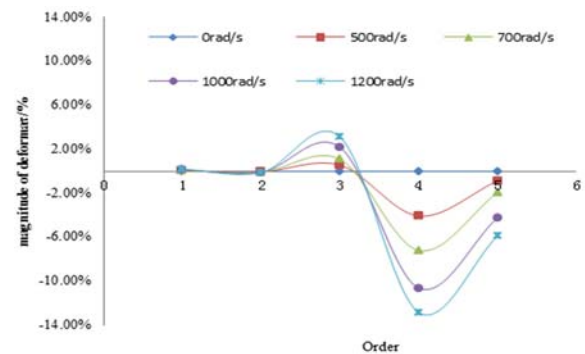


Fig. 3. The degree of deformation along X axis under the different speed.

As seen from Fig. 3, taking the deformation of blade along X axis at frequency of zero as a reference, the deformation of blade was proportional to the rotating speed at the same order of frequency. However, the influence degree on each order mode was different.

From the view of relative deformation, the first and third order modal deformations were positive with increasing speed. That is to say, the distortion of blade was appeared on two modes, which could increase the possibilities for rub impact between the tip and the casing, especially on the third order. By contrast, the second, fourth and the fifth modal deformations were negative, and generated bending deformation. The bending deformation was larger on the fourth and fifth orders, which demonstrated that the rub-impact had low probability of occurrence at these orders.

3.2. Vibration Analysis of Blade under the Thermal-Structure Coupling

In consideration of the actual working conditions, a blade analysis model of thermal-structure coupling was established. The thermal element of Solid70 and Shell131 was selected to establish thermo-mechanical coupling model. According to the gradual temperature change of blade, the linear temperature loads were applied to blade model, as shown in Fig. 4. At this

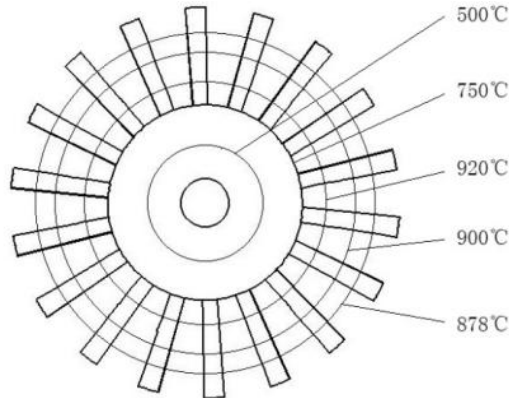


Fig. 4. Schematic of blade radial temperature.

point, temperature variation characteristics of blade material must be considered, and the data of Table 1 and Table 2 could be reset. Then, the thermal analysis was realized to obtain the temperature distribution of blade, as shown in Fig. 5.

Based on the thermal results, the different rotating speeds were loaded again. From solving results, we could research on all the modal characteristics combining the spin softening effect and thermal effect. The detailed characteristics were shown in Table 4.

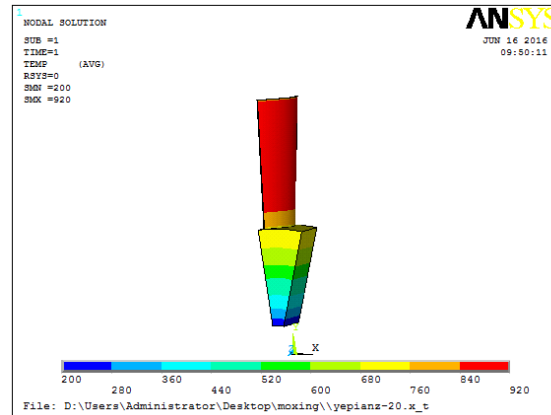


Fig. 5. Temperature distribution.

Table 4. Vibration mode of blade under the thermal structure coupling.

Order	Mode	Order (hz) (n=0)	Mode	Order (hz) (n=500)	Mode	Order (hz) (n=700)	Mode	Order (hz) (n=1000)	Mode	Order (hz) (n=1200)
1	T	317.23	T	339.19	T	357.77	T	394.41	T	423.55
2	B	569.9	B	579.84	B	588.94	B	607.71	B	623.35
3	T&B	1390.8	T&B	1432.2	T&B	1466.3	T&B	1536.0	T&B	1593.6
4	T&B	2064.4	T&B	2087.9	T&B	2096.6	T&B	2112.2	T&B	2123.6
5	T&B	2180.7	T&B	2211.3	T&B	2230.2	T&B	2272.5	T&B	2310.1

Note: n- the rotational speed of blade, rad/s; T- torsion; B- bending.

It can be seen from the Table 4, for the same order, the natural frequency of blade could increase with the increase of rotational speed under the thermal-structure coupling. Taking the first order as example, when the rotational speed raised from 0 rad/s to 1200 rad/s, the natural frequency changed from 317.23 Hz to 423.55 Hz, with the change range of 36.35 %. Compared with the result of simple centrifugal force, the variation was increased.

In comparison, we can also see that the change of each mode shape of blade was not very large at different speed. The first mode was also the torsional vibration along Y axis with smaller change, and the second mode was the bending vibration along X axis, too. From the third to sixth modes, the blade generated a combination of bending and torsion along X and Y axis.

In order to compare the influence of temperature field on vibration characteristics, it commissioned a study into the blade deformation along X axis at different speeds, as shown in Fig. 6.

Obviously, the first and third modal deformations were positive with the increasing speed, which intensified the possibility of rubbing, especially the third order. When rotational speed was 1200 rad/s, the deformation range of the first and third orders could reach to 4 %. That is to say, the distortion was more serious under the first and third modes, which could increase the possibilities for rub impact between the tip and the casing. More attention should be taken to pay attention to avoid producing fault in operation. However, modal deformations of the second, fourth and the fifth orders were negative with generating bending deformation, which demonstrated that there

was less likely to happen rub impact fault, especially at the fourth and the fifth. At that time, the engine could be in safe operation relatively.

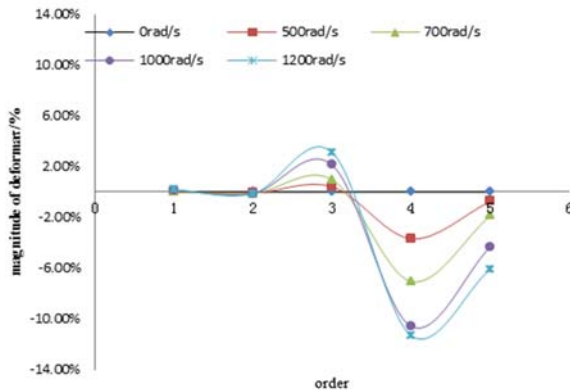


Fig. 6. The degree of deformation along X axis under the thermal-structure coupling effect.

3.3. Vibrating Characteristic of Blade with Temperature Rising

Finally, in conjunction with the above results, a conclusion had been drawn that increasing

temperature played an important role on the vibration characteristics of blade. The Table 5 were applied to shown specific difference of two fields on blades.

It can be seen from the Table 5, the natural frequency of blade could reduced with the increase of temperature. For every order at same rotating speed, the frequency of thermal-structure coupling dropped off comparing to that at single centrifugal field. Comparatively speaking, the larger change of frequency appeared the rotating speed of zero, with range about 3 % at each order. When the rotating speed changed from 0rad/s to 1200rad/s, the dropped range showed a downward trend in absolute value, with -3.37 % to -1.86 % at the first order, -3.33 % to -2.77 % at the second order, -3.38 % to -2.35 % at the third order, -3.41 % to -2.35 % at the forth order and -3.39 % to -2.60 % at the fifth order. According to the principle of the thermal-structure coupling influence, the resonance of whole structure should be avoided to reduce the amplitude of structural deformation and engine trouble.

Meanwhile, the increase of temperature brought larger deformation magnitude to the blades. According to actual working condition, the deformation of blade along X axis at 1200 rad/s was selected to compare the difference from centrifugal force field and thermal-structure coupling, which was shown in Table 6.

Table 5. Comparison of natural frequencies under thermal-structure coupling and centrifugal force field.

Order Speed	State	1	2	3	4	5
0 rad/s	centrifugal (Hz)	328.31	589.54	1439.5	2137.2	2257.2
	coupling (Hz)	317.23	569.9	1390.8	2064.4	2180.7
	deviation	-3.37 %	-3.33 %	-3.38 %	-3.41 %	-3.39 %
500 rad/s	centrifugal (Hz)	348.24	598.9	1474.8	2147.2	2275.5
	coupling (Hz)	339.19	579.84	1432.2	2087.9	2211.3
	deviation	-2.60 %	-3.18 %	-2.89 %	-2.76 %	-2.82 %
700 rad/s	centrifugal (Hz)	366.35	607.71	1507.8	2155.6	2294
	coupling (Hz)	357.77	588.94	1466.3	2096.6	2230.2
	deviation	-2.34 %	-3.09 %	-2.75 %	-2.74 %	-2.78 %
1000 rad/s	centrifugal (Hz)	402.19	625.91	1575.7	2170.8	2335.2
	coupling (Hz)	394.41	607.71	1536	2112.2	2272.5
	deviation	-1.93 %	-2.91 %	-2.52 %	-2.70 %	-2.68 %
1200 rad/s	centrifugal (Hz)	430.79	641.12	1631.9	2182	2371.8
	coupling (Hz)	423.55	623.35	1593.6	2123.6	2310.1
	deviation	-1.68 %	-2.77 %	-2.35 %	-2.68 %	-2.60 %

As can be seen from Table 6, the larger deformation was occurred at thermal-structure coupling field, when the rotational speed was 1200 rad/s. In contrast to other orders, the relative deformation of the fourth order was the biggest, reaching to 1.74 %. Therefore, the resulted obtained could demonstrated that it was more likely to happen rub-impact fault between blade and casing in a high speed, due to the increase of working environment temperature. This conclusion could provide the theoretical basis of thermal-structure coupling

research for blade-casing at high speed rotating machinery.

4. Conclusions

Under the condition of high speed rotation, the change of vibration mode characteristics of constrained blade was one of the main factors to cause the rub-impact failure of the blade and casing.

Table 6. Comparison of deformation under centrifugal force field and thermal-structure coupling.

Deformation \ Order	1	2	3	4	5
Centrifugal force(mm)	15.1252	15.6762	15.8563	12.6704	25.3826
Coupling(mm)	15.2396	15.7872	15.9821	12.8906	25.4533
Absolute deformation(mm)	0.1144	0.111	0.1258	0.2202	0.0707
Relative deformation	0.76%	0.71%	0.79%	1.74%	0.28%

In the paper, we laid emphasis to analyze the vibration modes of blade influenced from spin softening, centrifugal force field and thermal field on the basis of rotor dynamics and thermodynamic theory. It can be found that the spin softening effect changed the stiffness matrix and had a direct effect on vibration characteristics of constrained blades in high rotational process. The analyzed results demonstrated that the increase of rotating speed led to generate larger radial centrifugal force and enhance frequency at every order. Taking account to actual operational environment, a finite element model under thermal-structural field was established to get exact vibration characteristics of blade. It was worth noting that the blade frequency at same order would reduce with the increase of temperature. Thus larger deformation appeared when the temperature and speed increased. Especially, when the rotating speed reached to 1200rad/s in high temperature environment, the blade produced the larger torsion deformation along X axis at the third order. In the case, the gap between blade and casing could be reduced, and it was prone to happen to rub-impact fault and even engine failure, bringing huge economy losses. The obtained conclusion had an important meaning to study on transient rub impact between blade and casing of high speed rotating machinery.

Acknowledgements

This research was supported by Shan Dong Science and Technology Project (Grant No: J16LB01), University of Jinan Scientific Research Foundation.

References

- [1]. Jin Xiangming, Gao Peping, Cai Xianxin, et al., Analysis of integrated centrifugal impeller blade vibration reliability, *Journal of Aerospace Power*, 19, 5, 2004, pp. 610-613.
- [2]. C. M. Saravia, S. P. Machado and V. H. Cortínez, Free vibration and dynamic stability of rotating thin-walled composite beams, *European Journal of Mechanics A/Solids*, 30, 3, 2011, pp. 432-441.
- [3]. H Diken, K Alnefaie, Effect of unbalanced rotor whirl on blade vibrations, *Journal of Sound and Vibration*, 330, 14, 2011, pp. 3498-3506.
- [4]. Li Chuwang, Li Haiyun, Wang Che, et al., Study on frequencies and mode shapes of aeroengine turbine blades and its influencing factors, *Journal of Air Force Engineering University: Natural Science Edition*, 15, 1, 2014, pp. 5-9.
- [5]. Sun Qiang, Zhang Zhongping, Chai Qiao, et al., Temperature effect on vibration frequency of aeroenging compressor blade, *Chinese Journal of Applied Mechine*, 21, 4, 2004, pp. 137-139.
- [6]. Xu Zili, Pan Yongyue, Xiao Changjiang, et al., The influence of root-wards infiltrated vibration on its mode order in vase of interconnected blade triplets with "T" root, *Journal of Aerospace Power*, 26, 2, 2006, pp. 207-210.
- [7]. Yao Shixue. Study on dynamics of wind turbine blade based on spin softening, *Journal of Chinese Society of Power Engineering*, 31, 3, 2011, pp. 209-213.
- [8]. Xie Yonghui, Zhang Di, Numerical model for vibration characteristic of steam turbine blade with damped shroud, *Proceedings of the CSEE*, 25, 18, 2005, pp. 86-90.